Received: 1 February 2024 | Revised: 2 July 2024 | Accepted: 22 July 2024

IET Power Electronics

DOI: 10.1049/pel2.12756

The Institution of Engineering and Technology WILEY

CASE STUDY

Evaluation of maximum power point tracking methods for a marine current energy converter

Christoffer Fjellstedt | **Johan Forslund** | **Anders Goude** | **Karin Thomas**

Division of Electricity, Department of Electrical Engineering, Uppsala University, Uppsala, Sweden

Correspondence
Christoffer Fjellstedt, Division of Electricity, Department of Electrical Engineering, Uppsala University, Sweden.
Email: christoffer.fjellstedt@angstrom.uu.se

Funding information
StandUp for Energy

Abstract

Marine current power is attracting more attention as a renewable energy option. Similar to wind power, marine current power often requires a maximum power point tracking (MPPT) method to optimize power extraction from the free-flowing water. Research into MPPT methods for marine current power remains limited. Therefore, this paper presents a comprehensive investigation of MPPT methods for marine current power, building upon similar research in wind power. Three methods, namely the optimal tip speed ratio (OTSR), optimal torque (OT), and two variants of the perturb and observe (P&O) method, are explored. Using a simulation model developed for a specific marine current energy converter, where hydrodynamic calculations are coupled with electrical simulations, the study demonstrates that the OTSR method achieves MPPT with a comparably fast convergence time. After a change in water speed, the OTSR method achieves optimal operation within two turbine rotations. Additionally, the P&O methods are shown to achieve MPPT, albeit with a significantly longer convergence time. However, the P&O methods can be more convenient since no model of the system is required, and no water speed measurements are necessary. The proposed implementation of the OT method underperforms but positions the system close to the optimal operational point.

1 | INTRODUCTION

After hydropower, wind, and solar power collectively represent the most established renewable energy sources. Wind power constitutes 27% of the total global generation capacity, while solar power accounts for 31%, with the remaining share primarily sourced from conventional hydropower [1]. The increasing demand for electrical energy from renewable energy sources has prompted a search for additional green energy alternatives. Marine energy sources, such as wave power and marine current power, have demonstrated potential and are currently being developed as alternatives and complements to established renewable energy sources.

An important consideration when harnessing electrical power from wind and solar power is how the power extraction is optimized. Wind and solar are intermittent resources and can vary intensively from minutes to years [2]. Therefore, wind and solar power often require a maximum power point tracking (MPPT) strategy to optimize the extracted power [3, 4].

In wind power, two often discussed MPPT methods are the optimal tip speed ratio (OTSR) method and the optimal torque (OT) method [4–10]. Beyond these two strategies, a multitude of MPPT schemes can be found in the literature, many of which are based on a search method, for example, the perturb and observe (P&O) method [11]. An important distinction between the methods lies in the amount of required knowledge about the turbine and the types and quantity of sensors needed. The OTSR and OT methods require a deep understanding of the turbine's characteristics, while the P&O method does not require an accurate model of the turbine.

Wind power and marine current power are similar from a technological perspective. Technologies for marine current power are often based on a rotating turbine and generator [12]. Therefore, it is natural to draw on experiences from wind power when considering how to design technical solutions for marine current power. However, it cannot be assumed that a technical approach that is suitable for wind power by extension will be suitable for marine current power. Therefore, it is necessary

to study the implications of the solutions proposed for wind power for the specific characteristics of marine current power. However, the published research on MPPT methods for marine current power is still limited, particularly in journal publications. In [13], a review of MPPT methods is given based on research in wind power and one P&O method is simulated and analysed for a marine energy conversion system consisting of a tidal turbine, gearbox, permanent magnet synchronous generator (PMSG), rectifier and a buck converter connected to a load. It is concluded that the proposed MPPT method increases the power generated by the system. A simulation-based comparison of conventional PI control, high-order sliding mode control, and active disturbance rejection control is provided for a tidal stream turbine system in [14]. A model-based approach for MPPT for marine current turbines is investigated in [15]. The proposed concept is to exploit the predictability of the marine currents and instead of using sensors to determine the speed of the marine currents use a model for the marine current resource to determine the water speed at different times. A similar approach to sensorless control is proposed and discussed in [16] for a doubly-fed induction generator-based marine current turbine. In [17], a power limitation control at high tidal speeds for a marine current turbine with a PMSG is considered, and speed and torque MPPT control is additionally discussed. A sensorless MPPT approach for a marine current energy conversion system with an induction generator is considered in [18] and [19], where a growing neural gas network is used to estimate the water speed using the torque and the rotational speed of the generator. The estimated water speed is then used to generate the optimal rotational speed of the generator. In [20], a reinforcement learning-based algorithm is used for the MPPT for a tidal energy conversion system. In [21], an adaptive backstepping control method is used to achieve MPPT. The proposed method compensates for disturbances and uncertainties in the system. The method was supplemented with fuzzy logic control, allowing adjustments to the parameters of the adaptive backstepping control in real-time to enhance performance. Another example of applying a machine learning approach to MPPT is provided in [22], where support vector regression is used. The method is sensorless in that no water speed measurements are needed. The power is maximized by using a relation between the generator power and the generator speed, which has been constructed offline by the support vector regression. In [23], a P&O MPPT method was evaluated for a three-bladed vertical axis marine current turbine, using both a laboratory prototype and simulations. The P&O MPPT method was shown to have good performance both in the experimental tests and in the computer simulations. In [24], two active disturbance rejection control approaches with OTSR control are proposed for a marine current turbine and evaluated in a simulation-based study. The proposed control approaches are compared with traditional PI control and sliding mode control, and it is shown that the active disturbance rejection control approaches can be more efficient compared with the conventional methods. In [25], strategies to smooth the power from marine current turbines in view of current speed variations due to swell effects are investigated. The conventional OTSR method, a modified OTSR method where a low-pass filter is used to filter the reference rotational speed of the turbine, and the OT method were considered in the study. Using simulations, it was shown that all three methods are efficient, but the conventional OTSR method has the largest energy yield since it is the fastest in reaching the MPP. However, the power fluctuations are lower in the modified OTSR method and the OT method.

Many of the references discussed above consider a generic marine current energy converter or only discuss the MPPT method at a general level. Therefore, there is a need for more detailed studies on MPPT methods for specific marine energy converter technologies. The Division of Electricity at Uppsala University, Sweden, has developed a vertical axis marine current turbine. The turbine is deployed in the river Dalälven in Sweden and the test site comprises the turbine with a generator and an onshore measurement cabin with a grid connection system. The grid connection system is based on a back-to-back converter technology. The development and evaluation of the grid connection system are further presented in [26].

The system at the Söderfors test site has been evaluated in coupled electrical and hydrodynamic simulations in [27]. In this study, it has been shown that the results from the simulation model agree well with experimental results, except at low rotational speeds of the turbine. The electrical system model considered in the study encompasses only the generator side of the back-to-back converter. In the study in this paper, a full model of the electrical grid connection system, that is, the back-to-back converter, is coupled with the verified hydrodynamic model from [27]. The model is used to evaluate MPPT schemes from wind power research for the marine current power technology at the Söderfors test site.

In this paper, the OTSR method, the OT method, and the P&O method will be discussed. The theory will primarily be based on wind power research, but the implications of the methods for marine current power will be presented. Furthermore, four case studies using the coupled simulation model of the Söderfors marine current turbine will be presented. The case studies will demonstrate the performance of the OTSR, OT, and P&O methods on the turbine. The novelty of the study presented in this paper lies in applying these methods to a system with the specific characteristics of the Söderfors test site. More precisely, a slowly rotating turbine with large torque variations.

The paper is organized as follows. In Section 2, MPPT schemes for wind power are reviewed and discussed. The focus is on the methods OTSR, OT, and the P&O method. In Section 3, the MPPT methods are discussed with a focus on the characteristics of marine current power. In Section 4, the electrical system at the Söderfors test site is presented. Furthermore, the simulation model is presented. In Section 5, four case studies are presented where the simulation model is used to evaluate the OTSR, OT, and P&O methods for the marine current power system at the Söderfors test site. Finally, in Section 6, a summary of the paper is presented and the most important conclusions are given.

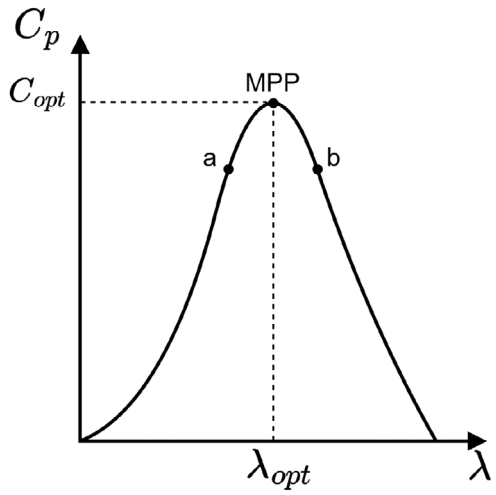

FIGURE 1 Typical power coefficient curve for a wind power turbine.

2 | MPPT METHODS IN WIND POWER

The main aim of an MPPT method in wind power applications is to adjust the rotational speed of the turbine in order to maximize the extracted power from the wind turbine for a given wind speed. Why this is the case will be explained in this section.

The mechanical power captured by a wind turbine can be described by the following equation:

$$P_{\mathrm{t}} = \frac{1}{2}\rho_{\mathrm{air}}\pi R^2 V_{\mathrm{wind}}^3 C_{\mathrm{p}}(\lambda,\beta), \tag{1}$$

where ρ_{air} is the density of air (often 1.225 kg/m^3 is used), R is the radius of the turbine in [m], V_{wind} is the wind speed in [m/s], and $C_{\mathrm{p}}(\lambda,\beta)$ is the wind turbine power coefficient. The power coefficient indicates how efficient the turbine is in transforming the power in the wind to mechanical power and is defined by

$$C_{\mathrm{p}} = \frac{P_{\mathrm{t}}}{P_{\mathrm{air}}}, \tag{2}$$

where P_{air} is the power in the wind. The maximum theoretical value of the power coefficient is given by the Lanchester–Betz limit, which is $16/27 \approx 59\%$ [28]. The actual maximum value of the power coefficient will depend on the properties of a specific wind turbine. As shown in Equation 1, the power coefficient is dependent on two parameters: the TSR (often designated by λ), and the blade pitch angle, β. The TSR is defined as the ratio between the tangential speed of the tip of the turbine blade and the velocity of the air, and it is given by the following equation:

$$\lambda = \frac{\omega_{\mathrm{t}} R}{V_{\mathrm{wind}}}. \tag{3}$$

For a given β, the power coefficient curve usually has a shape as shown in Figure 1. The power coefficient curve has a maximum value at a certain TSR. The maximum value represents the optimal power coefficient, that is, the maximum power point (MPP) where the power extracted from the wind is at the possible maximum value. In the figure, this point is indicated by C_{opt}. The optimal power coefficient is achieved at the optimal TSR (λ_{opt}).

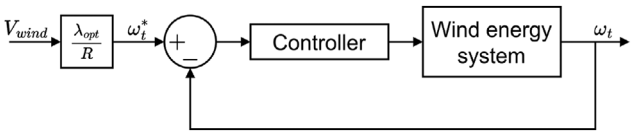

FIGURE 2 General operational principle of the OTSR method.

In wind power applications, MPPT strategies are often considered only for the region between the cut-in wind speed and the rated wind speed, commonly designated region 2 [6]. Beyond the rated wind speed, aerodynamic power control of the blades is employed, with the main techniques being passive stall, active stall, and pitch control [29].

MPPT algorithms have been used extensively in wind power applications and many methods have been proposed. One possible categorization of the methods is between indirect power control (IPC) methods and direct power control (DPC) methods [6, 10]. In the IPC methods, the control objective is to maximize the captured wind power, while the DPC methods aim to maximize the electrical power from the generator [6]. Additionally, hybrid methods can be considered where multiple methods are combined [6]. In the following sections, the OTSR method and the OT method, which can be classified as IPC methods, will be discussed. The DPC method P&O will also be considered, and finally, hybrid and intelligent methods will be discussed.

2.1 | OTSR in wind power

The general operational principle of the OTSR method is illustrated in Figure 2. Equation (3) is employed to calculate a reference value for the rotational speed of the turbine according to:

$$\omega_{\mathrm{t}}^* = \frac{\lambda_{\mathrm{opt}} V_{\mathrm{wind}}}{R}. \tag{4}$$

The reference value is compared with the actual rotational speed and the error is sent to a controller, for example, a PI controller. The OTSR method exhibits a fast response to wind speed variations [30]. The implementation of the method is also not theoretically complicated; only Equation (4) and measurements of the wind speed and rotational speed are needed. However, in practice, it can be a very difficult and expensive task to achieve accurate wind speed measurements [31]. For large wind turbines, the wind speed cannot be assumed to be the same over the whole wingspan of the turbine [31]. Furthermore, the OTSR method requires knowledge of the optimal TSR (λ_{opt}) which can be determined theoretically or experimentally [32]. The performance of the system will consequently be affected by the accuracy of the determination of the optimal

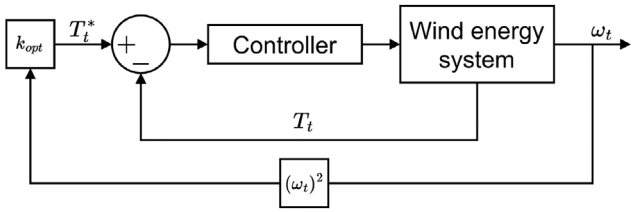

FIGURE 3 General operational principle of the OT method.

TSR. If this value is incorrect the performance of the turbine will be suboptimal.

2.2 | OT in wind power

In the OT method, the torque of the generator is controlled in order to achieve maximum power extraction from the turbine. If optimal operation of the turbine is assumed, $\lambda = \lambda_{\text{opt}}$ and $C_{\text{p}}(\lambda, \beta) = C_{\text{opt}}$, and the relationship $P_{\text{t}} = \omega_{\text{t}} T_{\text{t}}$ is used, Equation (1) can be rewritten as the following equation:

$$T_{\text{t}}^* = \frac{1}{2}\rho\pi R^5 \frac{C_{\text{opt}}}{\lambda_{\text{opt}}^3}\omega_{\text{t}}^2 = k_{\text{opt}}\omega_{\text{t}}^2, \tag{5}$$

where T_{t}^* is the reference torque given a rotational speed ω_{t}. The factor k_{opt} is a constant dependent on the properties of the turbine. The operational principle of the OT method is shown in Figure 3. The reference torque, T_{t}^*, is compared with the actual torque and the error is sent to a controller. Similar to the TSR method, the controller (which can be a PI controller) generates a control signal for the wind energy system. Unlike the TSR method, the OT method does not require wind speed data, making its control implementation simpler [9]. However, because the system does not react directly to changes in wind speed, the response time of the OT method is slower [9]. The OT method also requires accurate measurements of the torque and the rotational speed of the turbine. Furthermore, the factor k_{opt} is dependent on the mechanical status of the turbine and can change over time, which can affect the performance of the system negatively [4].

2.3 | P&O in wind power

The P&O method is based on the principle of imposing a perturbation on the system and observing the change in power. This method is widely used in wind energy systems [5]. In Figure 4, the concept of the method is illustrated. If the system is assumed to initially operate at point *a*, then the rotational speed of the turbine needs to be increased in order to move the system closer to the MPP. To achieve this, the rotational speed is increased by $\Delta\omega_{\text{t}}$ and the power output from the system is evaluated. The power is increased by ΔP and the system is now at operating point *b*. Since an increase in the rotational speed increases the power level, the rotational speed is

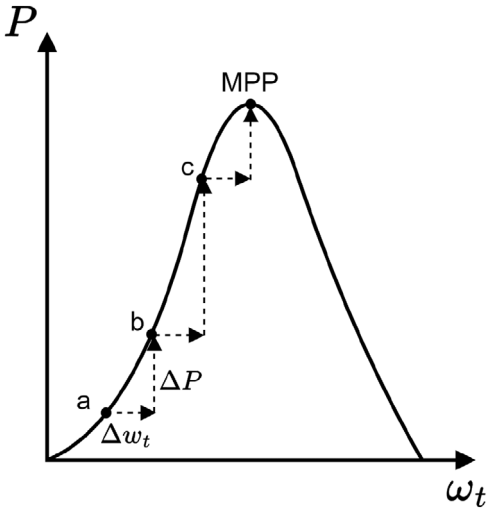

FIGURE 4 General operational principle of the P&O method.

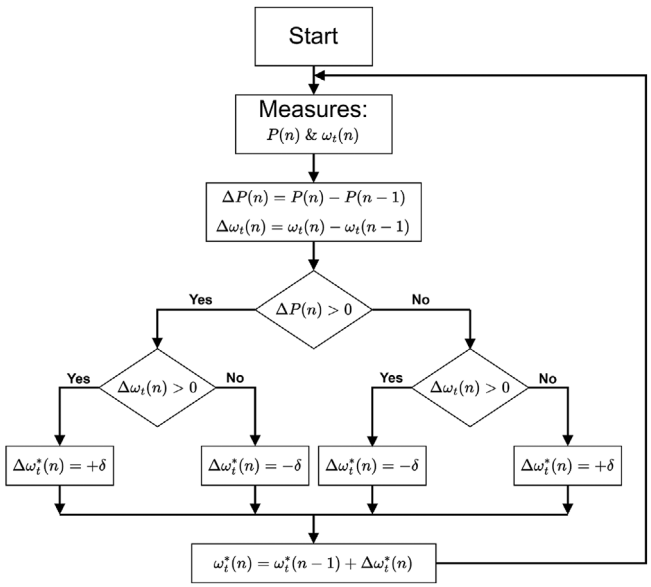

FIGURE 5 Flowchart of the P&O algorithm.

increased again. This is continued until no change in power can be observed, and the system can be assumed to be at the MPP. The approach is the same if the system operates to the right of the MPP. In this case, however, the rotational speed needs to be decreased.

An important consideration when using the P&O method is how to decide how much the control variable should be changed [11]. In Figure 4, this is illustrated by the incremental changes in the rotational speed of a wind turbine. A larger step size means that the system converges faster towards the MPP. However, in this case, the system can overshoot the MPP. A smaller step size makes it less probable that the MPP will be missed but increases the convergence time. Furthermore, the P&O method is sensitive to fast changes in wind speed [11].

In Figure 5, a flowchart of a P&O method is shown. Similar approaches can, for example, be found in references

TABLE 1 Comparison of the OTSR, OT, and P&O MPPT methods. The table is adapted from [6, 9].

Algorithm	Complexity	Convergence speed	Memory requirement	Wind speed measurement	Performance under varying wind conditions	Model dependent
OTSR	Simple	Fast	No	Yes	Moderate	Dependent
OT	Simple	Fast	No	No	Moderate	Dependent
P&O	Simple	Low	No	No	Moderate	Independent

[33, 34]. The first step in the considered method is to collect measurements of the output power from the system, $P(n)$, and the rotational speed of the turbine, $\omega_t(n)$. Then, the difference in power and rotational speed with regard to the earlier iteration is calculated. If the power was increased compared to the earlier iteration, and this was due to an increase in the reference value of the rotational speed of the turbine, then the reference value of the rotational speed, ω_t^*, is increased again by δ. On the other hand, if the increase in power was due to a decrease in the rotational speed, then the reference value of the rotational speed is decreased again. If Figure 1 is considered again, then it can be observed that the first case corresponds to the situation where the system operates at a point to the left of the MPP, that is, at point *a* in the figure. The second case, that is, when the rotational speed is further decreased, corresponds to point *b* in the figure. If the power is decreased by the perturbation, the change in the reference value of the rotational speed is the opposite of the described.

2.4 | Comparison of the MPPT methods for wind power

In many publications where MPPT methods are discussed, a comparison of the methods is presented. See, for example, references [4–6, 8, 9]. The results of the comparisons are often similar, but the wording can differ between the publications. In Table 1, some generalized characteristics of the MPPT methods are given. The table is adapted from [6, 9]. The column "model dependent" indicates if the method requires a model of the wind energy systems. For the OTSR method, a model is required in order to establish λ_{opt}. In the OT method, a model is required to determine a value for the k_{opt} factor. However, the P&O method does not require a correct model of the wind energy system.

2.5 | Other MPPT strategies in wind power

Hybrid strategies, where multiple methods are combined in order to improve the performance of the system, have been considered in the literature [6]. Furthermore, fuzzy-based, neural network-based, adaptive, and multivariable P&O methods have also been extensively investigated in the literature [6].

3 | MPPT METHODS AND MARINE CURRENT POWER

Even though a marine current power system has many similarities with a wind power system, differences should be considered in the MPPT design process. From a principle perspective, there are no obvious limitations to why the general principles of the MPPT methods discussed in Section 2, could not be used in marine current power. However, it is important to consider the specific characteristics of marine current power in order to evaluate the eventual limitations and possibilities.

Regarding the resource, that is, free-flowing water in the form of marine currents, it can be observed that marine currents, compared to wind, are highly predictable, though still variable in intensity [35]. The predictability of the marine currents opens the possibility of using, for example, a machine learning approach to predict the water speed without using water speed sensors. This approach has, for example, been considered in references [18–21]. It can generally be observed that using an approach where water speed measurements are necessary, for example, the OTSR method discussed in Section 2.1, results in the same issue as for wind power applications, that is, the problem of obtaining correct measurements of the water speed. For example, at the Söderfors test site, the water speed has been measured with two acoustic Doppler current profilers (ADCP) [36]. One of the ADCPs is located in front of the turbine and one after the turbine; therefore, the water speed at the turbine needs to be estimated. In [36], the water speed at the turbine was estimated by assuming the turbine to be located exactly at the midpoint between the ADCPs and that the change in the cross-section of the river is linear. The latter assumption is only reasonable since the turbine is located in a man-made channel. The issue of measuring an accurate water speed at a marine current turbine can be expected to be much more complicated in the open sea or channels with much more significant geometric variations.

Two important aspects where the conditions will differ significantly between wind and marine currents are the following [35]: firstly, the density of water is considerably higher than that of air, and secondly, the speed of water currents is much slower compared to wind speeds. Specifically, this implies that the turbine will rotate more slowly, resulting in the generator experiencing higher torque. Due to the slow rotation of the turbine, the rotational energy will be lower when compared to wind power applications. The control algorithms discussed in Section 2 need

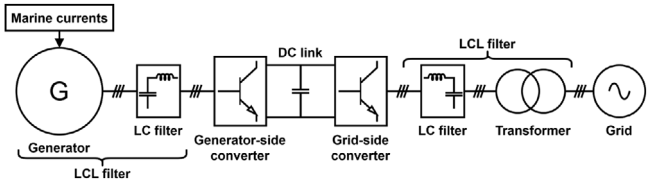

FIGURE 6 Overview of the electrical system at the Söderfors test site.

to be evaluated with regard to these conditions for a specific marine current energy converter technology. For instance, as the OT method utilizes the torque of the generator as a control variable, and this torque can be expected to be substantial in marine current power, it can become necessary to consider this in the controller design

As noted in Section 2, the P&O method can exhibit problems in performing when the wind speed is changing rapidly. Since the speed of marine currents is more stable and predictable than winds, the P&O method can be expected to be associated with fewer issues in marine current power compared to wind power.

4 | THE ELECTRICAL SYSTEM AT THE SÖDERFORS TEST SITE

The electrical system at the Söderfors test site is based on a back-to-back converter technology. An overview of the system is given in Figure 6. The energy in the free-flowing water is transformed into mechanical energy by the turbine, which, in turn, is transformed into electrical energy by the generator. The generator is a PMSG connected to the turbine in a direct-drive configuration, that is, no gearbox is used. The generator is connected to an onshore measurement cabin by an approximately 200 m long AC cable. The output from the generator is filtered with an LC filter in the measurement cabin. The filter, together with the inductance of the generator, constitutes an LCL filter. After the filter, the voltages and currents from the generator are transformed to DC quantities by an IGBT-based 2-level voltage source converter (2L-VSC). The generator-side converter is connected to the grid-side converter via a DC link. The grid-side converter is an IGBT-based 3-level voltage source converter (3L-VSC). The grid-side converter is connected to the distribution grid via an LC filter and a power transformer. The LC filter, together with the inductance of the transformer, forms an LCL filter. For more information about the development of the grid connection system at the Söderfors test site, refer to [26].

In the following sections, the details of the model that has been developed in order to describe the system at the Söderfors test site are presented. The aim of the model is to provide a comprehensive description of the system while being suitable for simulation. The presentation in the following sections will only offer an overview of the system and highlight the parts relevant to the current study. More details about the implementation of the model can be found in [37, 38].

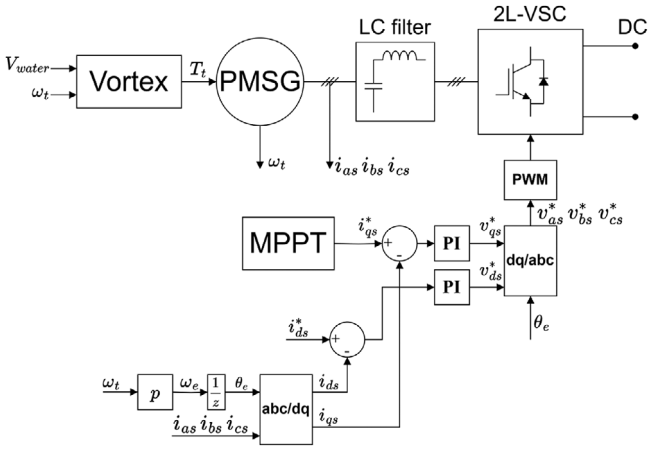

FIGURE 7 Generator side of the back-to-back converter with the vortex block for generating the torque for the generator.

4.1 | The generator side

The model of the generator side of the system is shown in Figure 7. The implemented control method is field-oriented control (FOC) with zero d-axis current. This method consists of two control loops, one to control the q-axis current and one to control the d-axis current. If the d-axis current is controlled to zero it can be shown the electromagnetic torque is given by the following equation [29]:

$$T_e = \frac{3}{2} p \Psi i_{qs}, \tag{6}$$

where Ψ is the rotor flux linkage, p is the number of pole pairs, and i_{qs} is the q-axis component of the stator current. From this equation, it can be concluded that by controlling the q-axis current, the electromagnetic torque of the generator can be controlled, which means that the speed of the turbine can be controlled. The reference value of the q-axis current is decided by the MPPT block. The MPPT strategy can be one of the methods from Section 2, for example, OTSR, OT, or P&O.

The parameters of the generator side of the system are given in Appendix A. The inductor of the LC filter is assumed to be non-ideal with a resistance value of 66 mΩ. LCL filters are associated with resonance issues, which can have an adverse effect on the controller [39]. One way to mitigate the resonance issue is to use a passive damping approach, where resistors are included in series with the capacitors [39]. In the model presented in this section, this passive damping approach is used. A suitable value for the damping resistor can be calculated using the following equation [40]:

$$R_d = \frac{1}{3\omega_{res} C_f}, \tag{7}$$

where C_f is the capacitance of the filter and ω_{res} is the resonance frequency of the LCL filter. Assuming that the generator-side LCL filter only consists of the generator inductance, and the capacitance and inductance of the LC filter, that is,

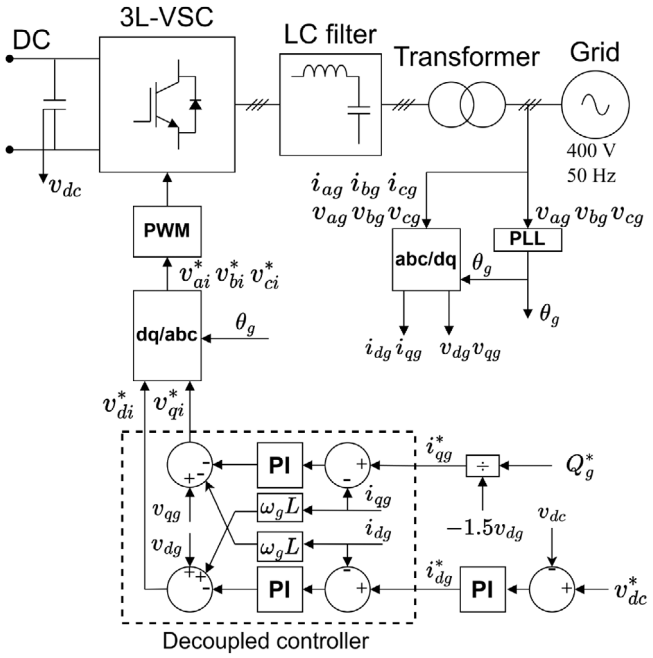

FIGURE 8 Grid side of the back-to-back converter.

neglecting the influence of the AC cable, and non-ideal properties of the components in the system, the resonance frequency can be calculated with the following equation [39]:

$$\omega_{\text{res}} = \sqrt{\frac{L_1 + L_2}{L_1 L_2 C_{\text{f}}}}, \tag{8}$$

where L_1 and L_2 are the inductances of the LCL filter.

Combining Equations (7) and (8), and using the parameter values from Appendix A, the value of the damping resistor can be calculated to be 3.49 Ω. The damping resistance can also be said to represent, to some extent, unknown resistances in the system due to the non-ideal properties of components, as well as resistance in cables and connectors.

The torque to the generator is generated by the vortex block in Figure 7. This block represents a two-dimensional free vortex method. It takes the rotational speed of the turbine and the water speed as inputs and gives the torque as output. The vortex method coupled with an electrical system has been validated for the marine current energy converter in Söderfors in [27]. The coupled simulations were shown to have good agreement with experimental data from the test site.

4.2 | The grid side

The grid side of the back-to-back converter is shown in Figure 8. The 3L-VSC is connected to the distribution grid via an LC filter and a power transformer. The distribution grid in the model has a line resistance of 34 mΩ and a line inductance of 0.5 mH [26]. The control method is voltage oriented control (VOC) with a phase-locked loop (PLL) scheme. The PLL scheme is the synchronous reference frame (SRF-PLL) method, which is more comprehensively explained in [41]. The parameter values of the grid side system can be found in Appendix A.

The controller is implemented with decoupled *d*- and *q*-axis components, which means that the reactive and active power can be controlled independently of each other [13]. The LC filter and the power transformer constitute an LCL filter. Since the system constitutes an LCL filter, it suffers from the issues arising from the occurrence of a resonance frequency. In order to mitigate the resonance issues, a damping resistor is included in the model. The value of the resistor is selected with Equation (7) and a modified version of Equation (8), see reference [38]. The value of the damping resistor is 2.31 Ω. The damping resistor of the grid side LCL filter can similarly, as in the case of the generator side filter, be said to represent parts of the resistive elements of the system that are not included in the model.

4.3 | MATLAB/Simulink implementation

The model presented in Sections 4.1 and 4.2 is implemented in MATLAB/Simulink. The Powergui components are used for the electrical components. The PI controllers are implemented as parallel discrete-time controllers. The model is simulated with a fixed step length. As discussed in Section 4.2, the torque on the generator is generated by the vortex.

5 | CASE STUDIES

The model presented in Section 4 is used to evaluate the OTSR, OT, and P&O methods. In the following sections, it is first described how the MPPT methods are implemented, and then the results from the simulations are shown.

5.1 | Implementation of the MPPT methods

5.1.1 | Implementation of the OTSR method

The power coefficient curve for the turbine is shown in Figure 9. The curve has been fitted from measurements on the turbine [42]. The optimal power coefficient is $C_{\text{opt}} = 0.26$ at an optimal TSR of $\lambda_{\text{opt}} = 3.05$. For the OTSR method, the optimal TSR is used with Equation 4 in order to generate a reference value for the rotational speed of the turbine given a certain water speed. The reference value is compared with the actual rotational speed, as illustrated in Figure 2, and the error is sent to a PI controller, which generates the *q*-axis reference current, i^*_{qs}.

5.1.2 | Implementation of the OT method

For the turbine at the Söderfors test site, the power captured by the turbine is given by the following equation:

$$P_{\text{t}} = \frac{1}{2}\rho_{\text{water}} A V^3_{\text{water}} C_{\text{p}}(\lambda), \tag{9}$$

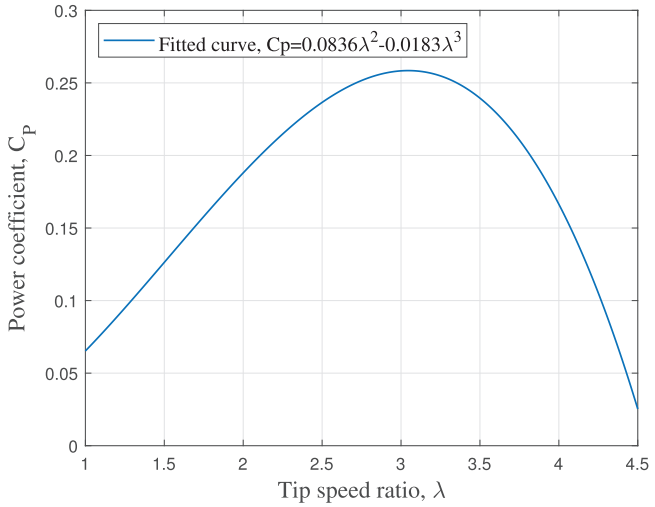

FIGURE 9 Power coefficient (C_p) curve fitted from measurements [42]. The optimal TSR derived from the fitted curve is $\lambda_{opt} \approx 3.05$, which corresponds to an optimal power coefficient of $C_p(\lambda_{opt}) \approx 0.26$.

where A is the cross-sectional area of the turbine, and ρ_{water} is the water density. The pitch of the turbine blades cannot be changed, and therefore, the power coefficient is only dependent on the TSR. The TSR is still given by Equation (3), but it is now defined as the velocity at the tip of the blades relative to the water speed, rather than the wind speed as before. If the TSR is inserted in Equation (9), the following equation is attained:

$$P_t = \frac{1}{2}\rho_{water} A R^3 \frac{C_{opt}}{\lambda_{opt}^3}\omega_t^3 = k_{opt}\omega_t^3. \tag{10}$$

And with $P_t = T_t\omega_t$:

$$T_t = k_{opt}\omega_t^2. \tag{11}$$

If the density of the water is assumed to be 997 kg/m^3 and the parameter values for the turbine from Appendix A are used together with the optimal TSR and the optimal power coefficient, then the optimal k-factor can be calculated as the following:

$$k_{opt} = \frac{1}{2}\cdot 997 \cdot 21 \cdot 3^3 \frac{0.26}{3.05^3} \approx 2590. \tag{12}$$

Equation (6) can be rewritten and combined with Equation (11) to generate a q-axis reference current for the controller:

$$i_{qs}^* = \frac{2}{3p\Psi} k_{opt}\omega_t^2. \tag{13}$$

In the implemented OT control method, Equation (13) is used directly as the reference current. This approach is similar to the general operational principle of the OT method illustrated in Figure 3. However, using Equation (13), no additional PI controller is required.

5.1.3 | Implementation of the P&O method

The P&O method, as illustrated in Figure 5, is implemented. The power at different parts of the system can be considered, such as the power on the DC link or the three-phase output power from the generator. Two other cases are considered here: 1) the mechanical power to the generator, $P_t = T_t\omega_t$, and 2) the power injected into the distribution grid, calculated using the dq-components of the grid currents and voltages, expressed as $P_g = \frac{3}{2}(v_{dg}i_{dg} + v_{qg}i_{qg})$.

The reference value for the rotational speed, $\omega_t^*(n)$, generated by the P&O algorithm is compared with the actual rotational speed, and the error is sent to a PI controller, which generates the q-axis reference current, i_{qs}^*.

The rotational speed of the turbine is not changed immediately when the reference value is changed. Therefore the system is allowed 2 s to settle. Furthermore, the torque and rotational speed of the turbine oscillate, which depends on the five-bladed construction of the turbine. In order to account for this and eventual noise, the mean value of the power and the rotational speed is used. The mean value is calculated for 8 s. Therefore, the time between each iteration of the algorithm is 10 s.

If the change in power is very low between two steps of the rotational speed, then it is reasonable to assume that the system is close to the MPP. In this situation, the difference in power can possibly depend on other factors than an actual difference in power, for example, noise. Therefore, it is imposed that the rotational speed is only changed when $|\Delta P| > d$, where d is a predefined limit, and in this case, 20 W.

An important design parameter in the algorithm is the size of the change in the reference value of the rotational speed, δ. The nominal rotational speed of the generator is 1.57 rad/s, and therefore, in order not to miss the optimal value, a step length of 0.01 is selected. This choice can result in a slow convergence time but decreases the risk of missing the MPP.

5.2 | Simulation results

The simulations are performed in a similar way for all three MPPT methods. However, due to differences in settling times between the methods, various simulation durations are employed. All simulations start at a water speed of 1.2 m/s. After allowing time for the simulation to settle, the water speed is then increased to 1.3 m/s. It is important to note that this sudden increase in water speed does not represent a realistic change; rather, it is used exclusively to assess the performance of the controllers. This includes evaluating their ability to respond to sudden changes in water speed and accurately track the MPP.

The following four mechanical variables are evaluated: rotational speed (ω_t in [rad/s]), torque (T_t in [Nm]), TSR ([−]), and C_p ([−]). The TSR is calculated using Equation (3) with the water speed, and the power coefficient is calculated using Equation (2). Additionally, the following electrical variables are evaluated: the reference q-current (i_{qs}^* in [A]) and the three-phase generator currents (I_{abc} in [A]).

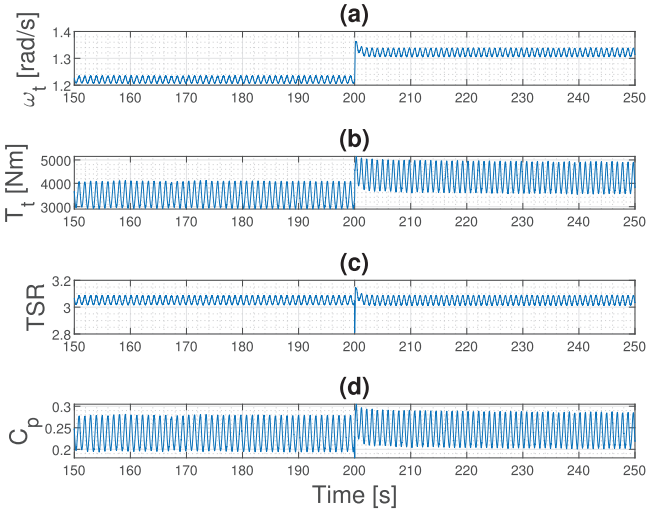

FIGURE 10 Considered mechanical variables for the system with OTSR MPPT control: (a) rotational speed, ω_t [rad/s], (b) torque, T_t [Nm], c) TSR [−], and d) Power coefficient, C_p [−].

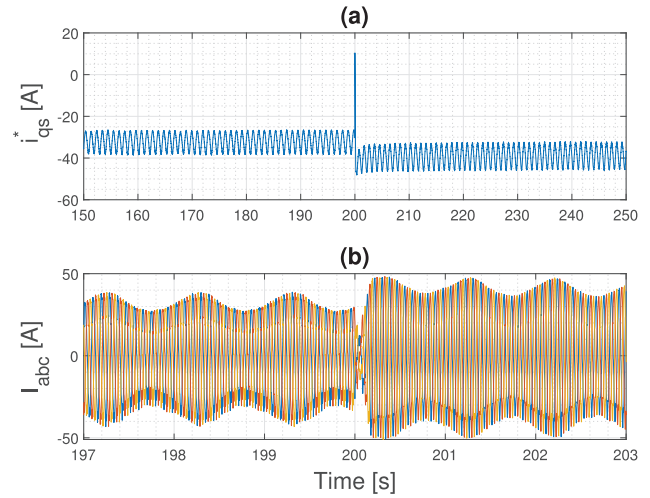

FIGURE 11 Considered electrical variables for the system with OTSR MPPT control: (a) q-axis reference current, i^*_{qs} [A], and (b) Three-phase generator currents, I_{abc} [A].

The gains of the PI controllers were set by trial and error.

5.2.1 | Simulation of the OTSR method

The OTSR method is simulated for 400 s. At 200 s, the water speed is increased from 1.2 to 1.3 m/s. In Figure 10, the evaluated mechanical variables are shown and in Figure 11, the electrical variables are shown. It should first be observed that the torque and rotational speed in Figures 10a and 10b, respectively, experience oscillations, which are due to the five blades of the turbine. Since the TSR and the power coefficient in Figures 10c and 10d are calculated using the rotational speed and the torque, the oscillations are also observed in these variables. Because of the oscillations, it is suitable to consider the mean values of the variables, which are shown in Table 2. In this table, the peak-to-peak values of the variables are also shown within the parenthesis. The values have been calculated for the time periods from 160 to 180 s and from 220 to 240 s.

TABLE 2 Mean and peak-to-peak values of rotational speed, torque, TSR, C_p, and the q-axis reference current with OTSR MPPT control. Values are provided for both before and after the step in water speed.

Variable	Before the step mean (peak-to-peak)	After the step mean (peak-to-peak)
Rotational speed, ω_t [rad/s]	1.22 (0.029)	1.32 (0.034)
Torque, T_t [kNm]	3.49 (1.20)	4.22 (1.43)
TSR [−]	3.05 (0.074)	3.05 (0.077)
C_p [−]	0.24 (0.086)	0.24 (0.088)
q-axis reference current, i^*_{qs} [A]	−32.25 (11.94)	−38.96 (14.09)

From the perspective of the MPPT controller, the TSR and C_p variables are the most important. Assuming the power coefficient curve in Figure 9 to be correct, the power extracted from the free-flowing water is maximized when the system is operated at a TSR of $\lambda_{opt} = 3.05$ and this corresponds to a power coefficient of 0.26. As shown in Table 2, the mean value of the TSR is 3.05 before and after the step. Similarly, the power coefficient settles to the same value before and after the step at 0.24. It can therefore be concluded that the controller is able to steer the system towards the assumed optimal TSR, but the power coefficient is slightly smaller than the assumed optimal value. An explanation for this could be that the optimal C_p has been calculated from a fitted curve based on experimental data. It is possible that the polynomial fitted curve does not precisely capture the peak value of the power coefficient curve. Another likely explanation could be that the experimental values do not exactly correspond to the theoretical values provided by the simulation model.

Considering again the TSR and C_p in Figure 10, it can be observed that the convergence to the optimal TSR and the corresponding C_p after the step in the water speed is very fast. Within 10 s the turbine has settled into a steady state at the optimal TSR. Considering the mean value of the rotational speed of the turbine after the step (1.32 rad/s), this corresponds to just above two turns of the turbine. A similar behaviour to that of the TSR can be observed for the rotational speed, the torque, and the q-axis reference current in Figure 11a. At the step, a significant transient can be observed in the q-reference current, but the current still stabilizes to a new steady state value.

The three-phase generator currents are shown in Figure 11b. The large oscillations are due to the five-bladed structure of the turbine. When the water speed increases, the amplitudes of the currents increase as more electrical power is transported from the generator to the grid.

It can be concluded that the OTSR MPPT method is able to achieve its control objective in steering the system towards the assumed optimal TSR value, according to the input parameters

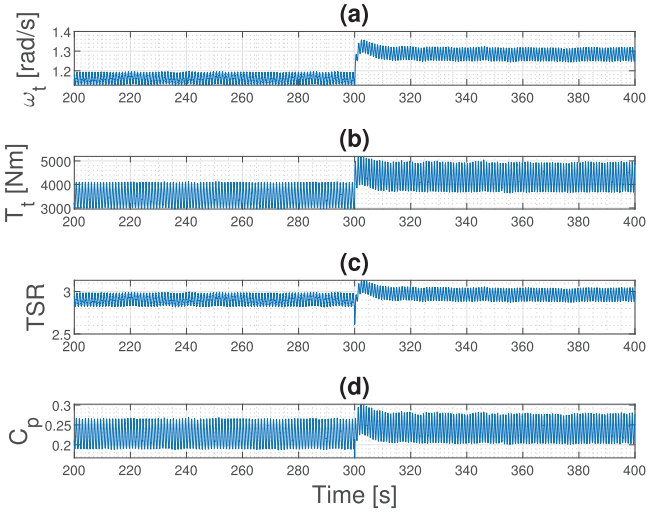

FIGURE 12 Considered mechanical variables for the system with OT MPPT control: (a) rotational speed, ω_t [rad/s], (b) torque, T_t [Nm], (c) TSR [−], and (d) Power coefficient, C_p [−].

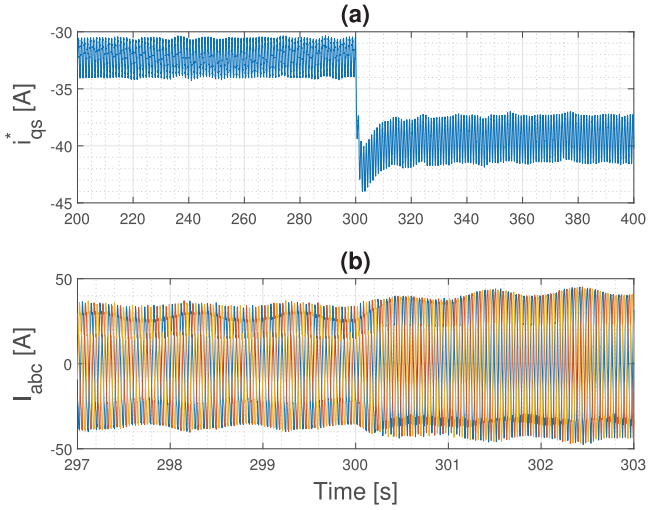

FIGURE 13 Considered electrical variables for the system with OT MPPT control: (a) q-axis reference current, i^*_{qs} [A], and (b) three-phase generator currents, I_{abc} [A].

to the controller. The method exhibits a fast response to changes in water speed. The controller is capable of achieving stable operation even in the presence of oscillations in the rotational speed of the turbine.

5.2.2 | Simulation of the OT method

The OT method is simulated for 800 s and the water speed is increased at 300 s. In Figure 12, the considered mechanical variables are shown for a time period of 200 s centered around the step in water speed. The electrical variables are shown for the same time period in Figure 13 and mean and peak-to-peak values calculated for the time periods 220 to 240 s and 360 to 380 s are given in Table 3.

TABLE 3 Mean and peak-to-peak values of rotational speed, torque, TSR, C_p, and the q-axis reference current with the OT MPPT control. Values are provided for both before and after the step in water speed.

Variable	Before the step mean (peak-to-peak)	After the step mean (peak-to-peak)
Rotational speed, ω_t [rad/s]	1.16 (0.069)	1.28 (0.075)
Torque, T_t [kNm]	3.50 (1.16)	4.25 (1.31)
TSR [−]	2.90 (0.17)	2.96 (0.17)
C_p [−]	0.23 (0.080)	0.24 (0.079)
q-axis reference current, i^*_{qs} [A]	−32.26 (3.84)	−39.25 (4.61)

As can be observed in Figures 12c and 12d together with the values in Table 3, the OT method does not achieve the assumed optimal TSR or C_p within the considered time frame. After the step, the power coefficient is 0.24 and the TSR is 2.96. Before the step, the values are slightly smaller at 0.23 and 2.90, respectively. Since the optimal k-factor, k_{opt}, is calculated with the assumption that the power coefficient curve in Figure 9 exactly corresponds to the description of the system given by the vortex it is possible that a systematic error is introduced if these do not exactly match each other. However, in that case, the TSR before and after the step would still be identical if the controller was able to achieve operation at the reference torque calculated with the k_{opt} factor, which is not the case now. A possible explanation for this is that the controller is badly tuned. A more sophisticated tuning method for the PI gains, or possibly a completely different control approach, could potentially improve the performance of the controller. However, even though the controller in this case is not able to achieve optimal operation according to the assumed optimal operational point, it can be noted that the controller can position the system at a rotational speed near the assumed optimal point. Moreover, the power coefficient after the step increase in water speed attains the same value as in the OTSR MPPT case.

5.2.3 | Simulation of the P&O method with P_t

The P&O method with $P_t = \omega_t T_t$ as the considered power reference is simulated for 800 s, and the water speed is increased at 300 s. The mechanical variables are shown in Figure 14, and the electrical variables are shown in Figure 15. The mean and peak-to-peak values are given in Table 4 and are calculated for the time periods of 250 to 290 s and 760 to 800 s.

Since the P&O method is model-free it will optimize the power conversion only with regard to the effect on the considered power reference by a change of the control variable, which is the rotational speed of the turbine. Therefore, it is not necessarily the case that the assumed optimal TSR and C_p are achieved. If the power coefficient, as fitted on the experimental data in Figure 9, does not exactly correspond to the model of the system, another MPP can be found. If the power coefficient

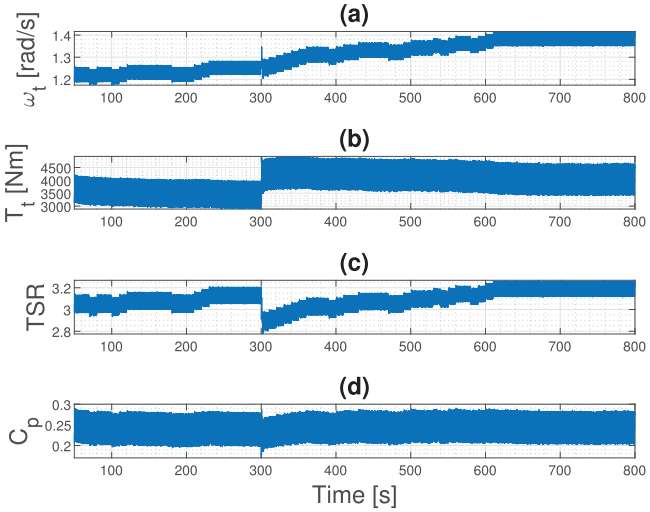

FIGURE 14 Considered mechanical variables for the system with P&O MPPT control with P_t as power reference: (a) rotational speed, ω_t [rad/s], (b) torque, T_t [Nm], (c) TSR [−], and (d) power coefficient, C_p [−].

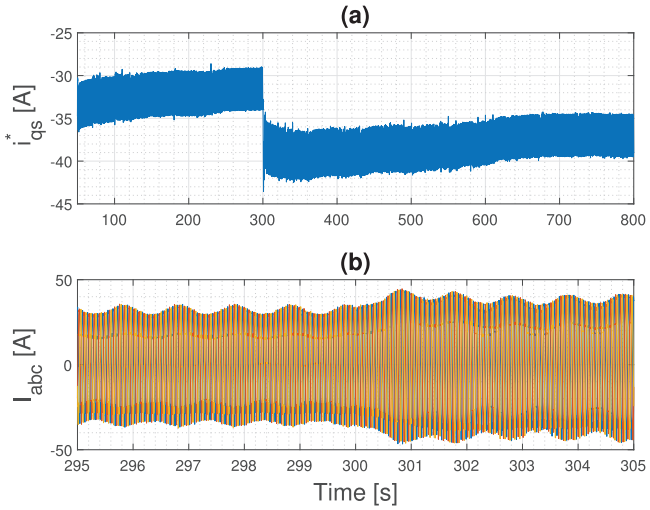

FIGURE 15 Considered electrical variables for the system with P&O MPPT control with P_t as power reference: (a) q-axis reference current, i^*_{qs} [A], and (b) Three-phase generator currents, I_{abc} [A].

TABLE 4 Mean and peak-to-peak values of rotational speed, torque, TSR, C_p, and the q-axis reference current with the P&O MPPT control with P_t as the considered power reference. Values are provided for both before and after the step in water speed.

Variable	Before the step mean (peak-to-peak)	After the step mean (peak-to-peak)
Rotational speed, ω_t [rad/s]	1.25 (0.064)	1.38 (0.066)
Torque, T_t [kNm]	3.41 (1.12)	3.99 (1.28)
TSR [−]	3.13 (0.16)	3.18 (0.15)
C_p [−]	0.24 (0.086)	0.24 (0.083)
q-axis reference current, i^*_{qs} [A]	−31.48 (5.16)	−36.86 (5.39)

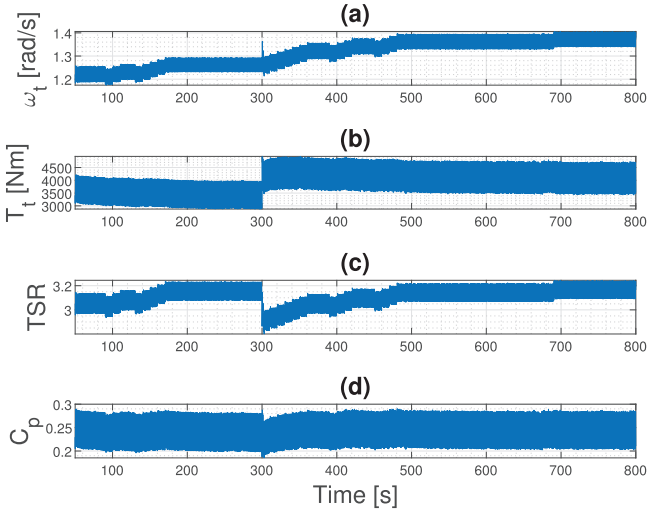

FIGURE 16 Considered mechanical variables for the system with P&O MPPT control with P_g as the considered power reference: (a) rotational speed, ω_t [rad/s], (b) torque, T_t [Nm], (c) TSR [−], and (d) power coefficient, C_p [−].

in Table 4 is studied, it can be concluded that when the system is at a steady state it reaches the same value of 0.24 both before and after the step in water speed. The TSR at these points is 3.13 and 3.18, respectively. The power coefficient is a bit lower than the assumed optimal of 0.26, but very close and actually the same value that was achieved in the OTSR method and in one instance for the OT method.

An observation that can be made for the P&O method is that the convergence time is comparably very slow. If the TSR after the step in Figure 14c is considered, it can be observed that it takes 300 s before a new steady state is found, which can be compared to below 10 s for the OTSR method. The same tendency is visible in the power coefficient, but here, around 400 s appears to be needed.

It should be observed that the convergence time is dependent on how the P&O method is implemented. In the proposed implementation a step length of 0.01 was used as the change of the control variable. The convergence time could possibly be improved if this value was increased. However, the risk in this case is that the MPP is missed. Furthermore, in the proposed implementation, the mean value of the power is used to evaluate the power level. This value is calculated every 10 s using an 8 s sample. The convergence speed could, therefore, possibly be improved if the time between each iteration of the algorithm was decreased.

5.2.4 | Simulation of the P&O method with P_g

The P&O method with P_g as the considered power reference is simulated for 800 s, and the water speed is increased at 300 s. The mechanical variables are shown in Figure 16, and the electrical variables are shown in Figure 17. The mean and peak-to-peak values are given in Table 5 and are calculated for the time periods of 250 to 290 s and 760 to 800 s.

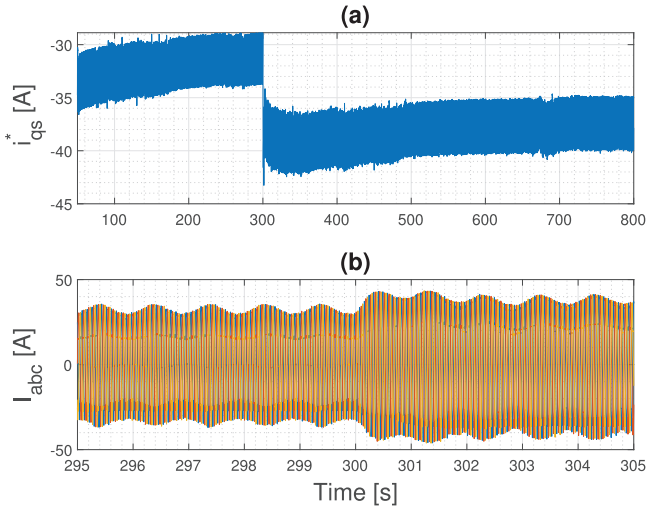

FIGURE 17 Considered electrical variables for the system with P&O MPPT control with P_g as the considered power reference: (a) q-axis reference current, i^*_{qs} [A], and (b) three-phase generator currents, I_{abc} [A].

TABLE 5 Mean and peak-to-peak values of rotational speed, torque, TSR, C_p, and the q-axis reference current with the P&O MPPT control with P_g as the considered power reference. Values are provided for both before and after the step in water speed.

Variable	Before the step mean (peak-to-peak)	After the step mean (peak-to-peak)
Rotational speed, ω_t [rad/s]	1.26 (0.064)	1.37 (0.066)
Torque, T_t [kNm]	3.40 (1.11)	4.04 (1.31)
TSR [−]	3.15 (0.16)	3.16 (0.15)
C_p [−]	0.24 (0.084)	0.24 (0.084)
q-axis reference current, i^*_{qs} [A]	−31.33 (5.29)	−37.30 (5.40)

The result from using the power injected into the distribution grid as the considered power level is similar to the case where mechanical power was used. The convergence time is comparably long, but as already observed, this will depend on how the P&O method is implemented. The power coefficient settles to a mean value of 0.24 both before and after the step in water speed, which is exactly the same value as for the OTSR method and the P&O method with P_t. If the mean and peak-to-peak values for the method with the mechanical power as reference in Table 4 are compared with the values for the method with the grid side power in Table 5, it can be concluded that the results are very similar. Therefore, regarding the efficiency of the methods, they can be perceived as interchangeable. The choice between the methods must therefore be made with regard to other factors, such as the need for additional sensors.

Since the dq-components are already available in the grid-side controller, using the grid-side power as a reference appears as an efficient use of the variables in the system. The speed of the generator needs to be measured or estimated in order to operate the generator-side controller. Therefore, both variables that are needed to implement the P&O method with P_g as the considered power reference are attainable without the need for extra sensors. On the other hand, for the P&O method with mechanical power as a reference, a torque sensor will be required.

5.3 | Comparison and discussion of the simulation results

From the simulations, it can be concluded that the OTSR method and the P&O methods have the best performance in steady state. The methods are able to achieve a power coefficient of 0.24 before and after the increase in water speed. However, the convergence time for the P&O methods is much slower than that of the OTSR method. On the other hand, two important advantages of the P&O methods compared with the OTSR method are that no accurate model of the turbine is required and no water speed measurements are needed.

The steady-steady state performance of the OT method was almost as good as the OTSR method and the P&O methods. However, the OT method showed a lower power coefficient of 0.23 before the step. After the step, the power coefficient was 0.24. The convergence time was longer for the OT method compared to the OTSR method but not as long as for the P&O methods.

As noted above, none of the methods achieve the assumed optimal power coefficient. The reason for this is probably that the assumed optimal values are based on measurements of the actual turbine, and these measurements do not completely correspond to the description of the system given by the proposed simulation model. However, since all methods, except the OT method in one instance, achieve the same maximal power coefficient, it is reasonable to believe that this value is the maximum power coefficient for the considered simulation model. This point is further supported by the fact that the P&O method with P_t as power reference achieves this value without any prior knowledge of the turbine parameters and by tracking the MPP directly with regard to the power of the turbine.

6 | SUMMARY AND CONCLUSIONS

The MPPT methods OTSR, OT, and P&O have been presented and discussed, with an emphasis on marine current power applications. Special focus has been placed on the characteristics of the marine current energy converter at the Söderfors test site in Sweden. It has been argued that the P&O method may be easier to implement in marine current applications, as the resource, free-flowing water in marine currents, is more stable than wind. Furthermore, it has been suggested that the general characteristics of marine current power, with low water speed and high torque, need to be considered in the design process of the MPPT method.

The OTSR, OT, and P&O methods have been evaluated for the specific technology at the Söderfors test site using a simulation model where hydrodynamic calculations and an electrical model are coupled. As a reference for the performance of the methods, an optimal power coefficient with a corresponding TSR, which is based on measurement data, has been used. None of the methods are able to achieve the optimal power coefficient based on the measurement data, which is probably due to a discrepancy between the simulation model and the measured values. However, all methods, except the OT method in one instance, achieve the same maximum power coefficient, and therefore, it is argued that this value is probably the maximum value for the considered simulation model.

The results from the simulations show that the OTSR method is very efficient in achieving MPPT for the considered turbine. The convergence time to achieve a rotational speed of the turbine at which the system operates at the optimal TSR is approximately two turns of the turbine after a step is applied to the water speed. The OTSR method would, however, require correct water speed measurements, which can be difficult to attain in practice. The OT method does not require water speed measurements. However, the method implemented in the case study in this paper was shown to underperform compared to the other methods. The power coefficient is, in one instance, smaller compared to the maximum attained by the other methods. A possible explanation for the offset is that periodic oscillations in the reference value for the PI controller make it difficult to tune the PI gains. The oscillations arise from the five-bladed structure of the turbine.

The P&O methods are also able to track the MPP. However, the convergence time is very long compared to the OTSR method, but the possibility of achieving MPPT without water speed measurements can outweigh this drawback.

AUTHOR CONTRIBUTIONS

Christoffer Fjellstedt: Conceptualization; data curation; formal analysis; investigation; methodology; project administration; software; validation; visualization; writing—original draft; writing—review and editing. **Johan Forslund**: Conceptualization; formal analysis; methodology; project administration; resources; validation. **Anders Goude**: Conceptualization; methodology; validation. **Karin Thomas**: Conceptualization; funding acquisition; project administration; supervision.

ACKNOWLEDGEMENTS

This work was supported by StandUp for Energy.

CONFLICT OF INTEREST STATEMENT

The authors declare no conflicts of interest.

DATA AVAILABILITY STATEMENT

Data will be made available on request.

ORCID

Christoffer Fjellstedt https://orcid.org/0000-0002-0413-604X
Johan Forslund https://orcid.org/0000-0003-1129-3825

REFERENCES

1. Renewable capacity highlights 2023. International Renewable Energy Agency (IRENA). https://www.irena.org/-/media/Files/IRENA/Agency/Publication/2023/Mar/IRENA_-RE_Capacity_Highlights_2023.pdf (2023). Accessed 17 Aug 2023
2. Edenhofer, O., Madruga, R.P., Sokona, Y.: Renewable energy sources and climate change mitigation. Intergovernmental Panel on Climate Change. https://www.ipcc.ch/site/assets/uploads/2018/03/SRREN_Full_Report-1.pdf (2012). Accessed 17 Aug 2023
3. de Brito, M.A.G., Galotto, L., Sampaio, L.P., de Azevedo e Melo, G., Canesin, C.A.: Evaluation of the main MPPT techniques for photovoltaic applications. IEEE Trans. Ind. Electron. 60, 1156–1167 (2013)
4. Cheng, M., Zhu, Y.: The state of the art of wind energy conversion systems and technologies: a review. Energy Convers. Manage. 88, 332–347 (2014)
5. Abdullah, M., Yatim, A., Tan, C., Saidur, R.: A review of maximum power point tracking algorithms for wind energy systems. Renewable Sustainable Energy Rev. 16, 3220–3227 (2012)
6. Kumar, D., Chatterjee, K.: A review of conventional and advanced MPPT algorithms for wind energy systems. Renewable Sustainable Energy Rev. 55, 957–970 (2016)
7. Kumar, M.B.H., Saravanan, B., Sanjeevikumar, P., Blaabjerg, F.: Review on control techniques and methodologies for maximum power extraction from wind energy systems. IET Renewable Power Gener. 12, 1609–1622 (2018)
8. Pande, J., Nasikkar, P., Kotecha, K., Varadarajan, V.: A review of maximum power point tracking algorithms for wind energy conversion systems. J. Mar. Sci. Eng. 9, 1187 (2021)
9. Zhang, X., Jia, J., Zheng, L., Yi, W., Zhang, Z.: Maximum power point tracking algorithms for wind power generation system: review, comparison and analysis. Energy Sci. Eng. 11, 430–444 (2023)
10. Le, X.C., Duong, M.Q., Le, K.H.: Review of the modern maximum power tracking algorithms for permanent magnet synchronous generator of wind power conversion systems. Energies 16, 402 (2022)
11. Mousa, H.H., Youssef, A.-R., Mohamed, E.E.: State of the art perturb and observe MPPT algorithms based wind energy conversion systems: a technology review. Int. J. Electr. Power Energy Syst. 126, 106598 (2021)
12. Bahaj, A.S.: Generating electricity from the oceans. Renewable Sustainable Energy Rev. 15, 3399–3416 (2011)
13. Wen, M., Ren, Y., Srikanth, N.: Review of maximum power point tracking algorithm for tidal turbine generator. In: Proceedings of the 3rd Asian Wave and Tidal Energy Conference (AWTEC) 2016, pp. 1–6. Nanyang Technological University, Singapore (2016)
14. Zhou, Z., Elghali, S.B., Benbouzid, M., Amirat, Y., Elbouchikhi, E., Feld, G.: Control strategies for tidal stream turbine systems – a comparative study of ADRC, PI, and high-order sliding mode controls. In: Proceedings of the IECON 2019-45th Annual Conference of the IEEE Industrial Electronics Society, pp. 6981–6986. IEEE, Piscataway, NJ (2019)
15. Paz, F., Ordonez, M.: Open-loop maximum power point tracking strategy for marine current turbines based on resource prediction. In: Proceedings of the 2013 IEEE Electrical Power & Energy Conference, pp. 1–6. IEEE, Piscataway, NJ (2013)
16. Elghali, S.B., Benbouzid, M., Charpentier, J., Ahmed-Ali, T., Gahery, J., Denis, A.: Modeling and MPPT sensorless control of a DFIG-based marine current turbine. In: Proceedings of the 2008 18th International Conference on Electrical Machines, pp. 1–6. IEEE, Piscataway, NJ (2008)
17. Zhou, Z., Scuiller, F., Charpentier, J.F., Benbouzid, M., Tang, T.: Power limitation control for a PMSG-based marine current turbine at high tidal speed and strong sea state. In: Proceedings of the 2013 International Electric Machines & Drives Conference, pp. 75–80. IEEE, Piscataway, NJ (2013)
18. Greco, L., Testa, C., Cirrincione, M., Pucci, M., Vitale, G.: Marine current turbine generator system with induction machine growing neural gas (GNG) MPPT based on sensorless sea speed estimation. In: Proc. 2014 IEEE Energy Conversion Congress and Exposition (ECCE), pp. 3901–3908. IEEE, Piscataway, NJ (2014)
19. Greco, L., Testa, C., Cirrincione, M., Pucci, M., Vitale, G.: Effectiveness of a GNG-based MPPT and related control system for marine current

turbines in unsteady operating conditions. In: Proceedings of the 2015 IEEE Energy Conversion Congress and Exposition (ECCE), pp. 1027–1034. IEEE, Piscataway, NJ (2015)
20. Ouyang, Y., Zhao, W., Wang, H.: Simulation and study of maximum power point tracking for rim-driven tidal current energy power generation systems. Energy Rep. 9, 792–801 (2023)
21. Shen, X., Xie, T., Wang, T.: A fuzzy adaptative backstepping control strategy for marine current turbine under disturbances and uncertainties. Energies 13, 6550 (2020)
22. Abo-Khalil, A.G., Alghamdi, A.S.: MPPT of permanent magnet synchronous generator in tidal energy systems using support vector regression. Sustainability 13, 2223 (2021)
23. Michas, M., Ugalde-Loo, C. E., Ming, W., Jenkins, N., Runge, S.: Maximum power extraction from a hydrokinetic energy conversion system. IET Renewable Power Gener. 13, 1411–1419 (2019)
24. Zhou, Z., Elghali, S.B., Benbouzid, M., Amirat, Y., Elbouchikhi, E., Feld, G.: Tidal stream turbine control: an active disturbance rejection control approach. Ocean Eng. 202(4), 107190 (2020)
25. Zhou, Z., Scuiller, F., Charpentier, J.F., Benbouzid, M.E.H., Tang, T.: Power smoothing control in a grid-connected marine current turbine system for compensating swell effect. IEEE Trans. Sustainable Energy 4(7), 816–826 (2013)
26. Apelfröjd, S., Ekström, R., Thomas, K., Leijon, M.: A back-to-back 2L-3L grid integration of a marine current energy converter. Energies 8, 808–820 (2015)
27. Forslund, J., Goude, A., Thomas, K.: Validation of a coupled electrical and hydrodynamic simulation model for a vertical axis marine current energy converter. Energies 11, 3067 (2018)
28. Burton, T., Jenkins, N., Sharpe, D., Bossanyi, E.: Wind Energy Handbook. 2nd ed., Wiley, Hoboken, NJ (2011)
29. Wu, B., Lang, Y., Zargari, N., Kouro, S.: Power conversion and control of wind energy systems. 1st ed., Wiley, Hoboken, NJ (2011)
30. Nasiri, M., Milimonfared, J., Fathi, S.: Modeling, analysis and comparison of TSR and OTC methods for MPPT and power smoothing in permanent magnet synchronous generator-based wind turbines. Energy Convers. Manage. 86, 892–900 (2014)
31. Thongam, J.S., Tarbouchi, M., Beguenane, R., Okou, A.F., Merabet, A., Bouchard, P.: An optimum speed MPPT controller for variable speed PMSG wind energy conversion systems. In: Proceedings of the IECON 2012-38th Annual Conference on IEEE Industrial Electronics Society, pp. 4293–4297. IEEE, Piscataway, NJ (2012)
32. Abdullah, M.A., Yatim, A., Tan, C.W.: A study of maximum power point tracking algorithms for wind energy system. In: Proceedings of the 2011 IEEE Conference on Clean Energy and Technology (CET), pp. 321–326. IEEE, Piscataway, NJ (2011)
33. Chishti, F., Murshid, S., Singh, B.: Development of wind and solar based AC microgrid with power quality improvement for local nonlinear load using MLMS. IEEE Trans. Ind. Appl. 55(11), 7134–7145 (2019)
34. Cortes-Vega, D., Ornelas-Tellez, F., Anzurez-Marin, J.: Comparative analysis of MPPT techniques and optimal control for a PMSG-based WECS. In: Proceedings of the 2019 IEEE 4th Colombian Conference on Automatic Control (CCAC), vol. 10, pp. 1–6. IEEE, Piscataway, NJ (2019)
35. Bahaj, A.S.: Generating electricity from the oceans. Renewable Sustainable Energy Rev. 15, 3399–3416 (2011)
36. Forslund, J., Lundin, S., Thomas, K., Leijon, M.: Experimental results of a dc bus voltage level control for a load-controlled marine current energy converter. Energies 8, 4572–4586 (2015)
37. Fjellstedt, C., Forslund, J., Thomas, K.: Simulations of the electrical system of a grid connected marine current energy converter. In: Proceedings of the 14th European Wave and Tidal Energy Conference, pp. 1–9.
38. Fjellstedt, C., Forslund, J., Thomas, K.: A comparison of AC and DC collection grids for marine current energy. Paper presented at the 15th European wave and tidal energy conference, Bilbao, Spain, 3–7 Sept 2023
39. Gomes, C.C., Cupertino, A.F., Pereira, H.A.: Damping techniques for grid-connected voltage source converters based on LCL filter: an overview. Renewable Sustainable Energy Rev. 81, 116–135 (2018)
40. Araujo, S.V., Engler, A., Sahan, B., Antunes, F.L.M.: LCL filter design for grid-connected NPC inverters in offshore wind turbines. In: Proceedings of the 2007 7th International Conference on Power Electronics, pp. 1133–1138. IEEE, Piscataway, NJ (2007)
41. Golestan, S., Guerrero, J.M., Vasquez, J.C.: Three-phase PLLs: a review of recent advances. IEEE Trans. Power Electron. 32, 1894–1907 (2017)
42. Lundin, S., Forslund, J., Goude, A., Grabbe, M., Yuen, K., Leijon, M.: Experimental demonstration of performance of a vertical axis marine current turbine in a river. J. Renewable Sustainable Energy 8(6), 064501 (2016)

How to cite this article: Fjellstedt, C., Forslund, J., Goude, A., Thomas, K.: Evaluation of maximum power point tracking methods for a marine current energy converter. IET Power Electron. 1–15 (2024). https://doi.org/10.1049/pel2.12756

APPENDIX A: SYSTEM PARAMETERS

In Tables A1 and A2 the parameters used in the study are shown. The tables are adapted from references [26, 37, 38].

TABLE A1 Turbine and generator parameters. The table is adapted from [26, 37, 38].

Turbine	
$C_p(\lambda_{opt})$	0.26 at $\lambda_{opt} = 3.05$
Type	Vertical axis
Rotor height	3.5 m
Rotor radius (R)	3 m
Turbine area (A)	$21 m^2$
Generator	
Type	PMSG
Power rating	7.5 kW
Nominal rotational speed	15 rpm
Minimum efficiency	80%
Number of poles	112
Rated voltage ($V_{LL,\,rms}$)	138 V
Rated stator current (rms)	31 A
Stator phase resistance	0.335 Ω
Armature inductance	3.5 mH
Flux linkage[a,b]	1.29 Wb
Inertia[b]	2445 kgm^2
Viscous friction coefficient[b]	1 Nms

[a]Assuming a constant flux.
[b]The values for flux linkage, inertia and viscous friction are estimates.

TABLE A2 Electrical system parameters. The table is adapted from [26, 37, 38].

Component	Parameters	Values
Cable	Resistance	0.524 Ω/km
	Inductance	0.24 mH/km
	Capacitance	0.45 μ F/km

(Continues)

TABLE A2 (Continued)

Component	Parameters	Values
Rectifier	Converter type	2L-VSC
	Modulation scheme	SPWM
	Switching frequency	4 kHz
	Harmonic LC filter	1.6 mH, 10 μF
	Damping resistance	3.49 Ω
DC link filter	Capacitor bank	16.5 mF
Inverter	Converter type	3L-VSC
	Modulation scheme	SPWM
	Switching frequency	6 kHz
	Harmonic LC filter	2.4 mH (66 mΩ) 10 μF
	Damping resistance	2.31 Ω
Transformer	Delta/Wye	400 V/230 V
	Power rating	7.5 kVA
	Primary resistance	0.7 Ω
	Secondary resistance	0.23 Ω
	Primary leak. inductance	0.9 mH
	Secondary leak. inductance	0.3 mH
	Magnetization resistance	8225 Ω
	Magnetization inductance	9.22 H
Grid	Three-phase symmetrical	400 V, 50 Hz
IGBT	Internal resistance	0.1 mΩ
	Forward voltage	1 V
Rectifier diode	Internal resistance	0.001 Ω
	Forward voltage	0.8 V
Snubber circuit	Snubber resistance	47 kΩ
	Snubber capacitance	470 nF